A Smoothed-Particle Hydrodynamics (SPH) Model for Machining of 1100 Aluminum

S. S. Akarca, W. J. Altenhof, and A.T. Alpas
Department of Mechanical, Automotive and Materials Engineering,
University of Windsor, 401 Sunset Avenue,
Windsor, Ontario, Canada, N9B 3P4

Abstract

The smoothed-particle hydrodynamics (SPH) technique was used to model experimentally observed large deformation behaviour of aluminum (1100 Al) during machining. The effectiveness of the SPH method in predicting the response of the 1100 Al workpiece during orthogonal machining has been assessed through a careful comparison with the experimentally measured stress/strain distribution within the chips formed during steady state cutting. An Eulerian numerical model, previously validated for machining of copper, was also used to evaluate the SPH model. Both the Eulerian and SPH models showed good overall correlation with the experimentally measured stress/strain distribution when an exponential stress-strain behaviour was utilized in modeling. The maximum predicted plastic strains utilizing an Eulerian and SPH solution approach were 7.5 and 8.0, respectively. When the CPU time requirements were considered, the SPH model was the suitable choice to model deformation processes during cutting with relatively good accuracy and approximately 2.75 times less cost compared to the Eulerian model.

Introduction

The finite element method (FEM) used in modeling high strain (and strain rate) deformation processes, including metal cutting, consist of two major approaches: i) the Lagrangian approach and ii) the Eulerian approach. However, during modeling of ductile materials subjected to orthogonal cutting, severe mesh distortion occurs due to large strains and strain rates generated in the material ahead of the tool tip, resulting in a degradation of the simulation accuracy. In the Lagrangian approach, to compensate for mesh distortion and disintegration, chip separation/breakage criterion, adaptive meshing and continuous re-meshing are generally utilized. Application of Eulerian and SPH techniques for simulation of the metal cutting processes is important since both of the techniques are capable of modeling large deformations observed in the machining processes without facing numerical problems caused by element distortions. Furthermore, in the application of these techniques in metal cutting, there is no need to determine physical or geometrical element separation-breakage criterions to model chip formation other than material deformation behaviour defined by material properties. This is an advantage over the modeling approaches using element separation techniques, which are valid only for the specific problem studied and the accuracy of which is dependent upon the criterion used and the degree of discretization utilized.

Some examples involving the application of the Eulerian finite element formulation in machining can be found in [1-5]. The work presented in references [1-5] indicate that application of an Eulerian element formulation to machining significantly aids in overcoming mesh deformation concerns and the need for mesh separation criteria.

Smoothed-particle hydrodynamics (SPH) has found application in the study of certain problems, where large mesh deformations leading to significant numerical problems are an important concern [6, 7]. Cleary et al. [7] utilized SPH to model mold filling in high-pressure die

casting and ingot casting and demonstrated the ability of the SPH method to simulate detailed filling patterns of large-scale automotive die castings. In order to assess the applicability of Eulerian and SPH formulations in penetration problems Schwer investigated the impact of a rigid cylindrical fragment into a concrete panel [8]. He concluded that both Eulerian and SPH methods could be utilized in penetration problems when the results of those models were compared with the predictions of a Lagrangian simulation with erosion criteria. However, Buyuk et al. [9] reported that SPH method is not as successful as Lagrangian and Eulerian methods in the simulation of a ballistic impact. Very recently, Limido et al. [10] have utilized the SPH technique in two dimensional modeling of orthogonal cutting, to simulate continuous and shear localized chip formation.

The objective of this work was to investigate the effectiveness of the SPH finite element method to model machining of aluminum. A comparison amongst the SPH numerical scheme, the Eulerian finite element approach, which the authors have previous experience with [5], and experimental observations has been completed. Aspects of the numerical models (both Eulerian and SPH) including geometry, boundary conditions, friction model and discretization were maintained consistent. Variations in the mathematical basis of element formulations, including a mesh fixed (Eulerian) method and a mesh-free particle approximation (SPH) technique, were applied.

Experimental Procedures

1100 aluminum (Al) samples (>99.5 wt % Al) received in the form of a hot extruded rod were machined into a tubular shape with 25.4 mm outer diameter and 3.0 mm wall thickness prior to the orthogonal cutting tests. Orthogonal cutting tests were performed on a standard lathe without using metal removal fluids (i.e. under dry cutting conditions). The cutting tool insert used was a SiAlON grade silicon nitride based ceramic cutter (Kennametal CNGA-432) with a rake angle of α = - 5°. The cutting speed was kept constant at v = 0.6 m/s. As the primary concern was to preserve the deformation microstructure generated during cutting, a low cutting speed was purposely chosen to minimize the effect that sudden reduction in speed during breaking might cause on the deformation microstructure generated during cutting. The feed rate used was f = 0.25 mm/rev.

In experimental studies, local values of plastic strains in the primary and the secondary deformation zones of machined 1100 Al were determined through a careful examination of metallographic sections taken from the material ahead of the tool tip, where orientation changes of the flow lines in the material and shear angles were used to calculate plastic strains. Variations of local flow stresses were estimated from microhardness measurements. Examination of the stresses and strains at each measurement location generated a stress/strain relationship for the 1100 Al material.

Numerical Models

Finite element simulations were performed using the finite element program LS-DYNA® [11] (version 971 release 7600.398). Simulations were completed on a cluster of 32 CPUs with an internal clock speed of 2.0 GHz for each processor. Each simulation had a termination time of 20 ms and only 2 CPUs were utilized per simulation. Total simulation time was approximately 88 hours for the models utilizing the Eulerian technique, whereas it was approximately 32 hours for the models employing the SPH approach. A mesh convergence study

was completed and it was determined that a mesh size of 0.0625 mm was appropriate for the machining simulations considered in this study. This characteristic length was also selected for the particle spacing in simulations utilizing the SPH solution method.

In the Eulerian model, the workpiece and airmesh consisted of 29,026 single-point integration Eulerian elements with single material and void. The geometry of the Eulerian elements were solid hexahedral type with an aspect ratio of unity. The workpiece in the SPH model consisted of 21,156 SPH particles. The initial number of neighbours per particle was increased from 150 to 200 in the simulations and standard particle approximation theory was used. There were a total of 59,480 nodes and 29,356 elements in the Eulerian model and a total of 21,758 nodes and 21,456 elements in the SPH model.

The cutting tool was discretized using 330 Belytschko-Tsay type Lagrangian formulation elements in both of the Eulerian and SPH models. A velocity of v = 0.6 m/s in the X direction was assigned to the cutting tool. This velocity and the rake angle of α= -5° were specified to match the experimental operating parameters. The depths of cut used in the simulations were 0.25 mm and corresponded to the feed rate used in the experiments. Three dimensional quadrilateral shell elements were implemented for the cutting tool with an aspect ratio varying from unity to approximately 5.

To reduce the computation time, a subset of the experimental configuration was considered in the numerical models: the workpiece, airmesh and cutting tool were discretized between two planes of XY symmetry. Hence, the thickness of the models was 0.0625 mm and nodes lying on the XY-planes of symmetry were restricted to move only within those planes. The bottom nodes of the workpiece were fully constrained from motion (Figure 1).

Behaviour of the material model used for the workpiece was based on the material data obtained directly from the cutting experiments. A regression analysis showed that the relationship between the experimental flow stress and equivalent plastic strain values obeyed an exponential work hardening law expressed in the form of a Voce type equation [12]:

$$\sigma = \sigma_s - (\sigma_s - \sigma_0)\exp\left(\frac{-\bar{\varepsilon}^p}{\varepsilon_c}\right) \tag{1}$$

where σ is the value of the equivalent flow stress; $\bar{\varepsilon}^p$ is the corresponding equivalent plastic strain; σ_s (302 MPa) is the saturation stress at which the work hardening rate becomes zero; σ_0 (140 MPa) is the flow strength of the material; and ε_c (1.4) is a constant. The Grüneisen equation of state (EOS) was employed to define the pressure-volume relationship of the 1100 Al material and the constants required for input in the Grüneisen equation of state were obtained from the work of Steinberg [13].

Since the deformation of the cutting tool was negligible compared to the workpiece, the tool was modeled as a rigid material. The density, shear modulus and Poisson's ratio of the workpiece were specified as 2.71 $Mg{\cdot}m^{-3}$, 27.0 GPa and 0.33, respectively. The properties of the cutting tool were specified as follows: density ρ = 3.20 $Mg{\cdot}m^{-3}$, Young's modulus E = 300.0 GPa, and Poisson's ratio ν = 0.25.

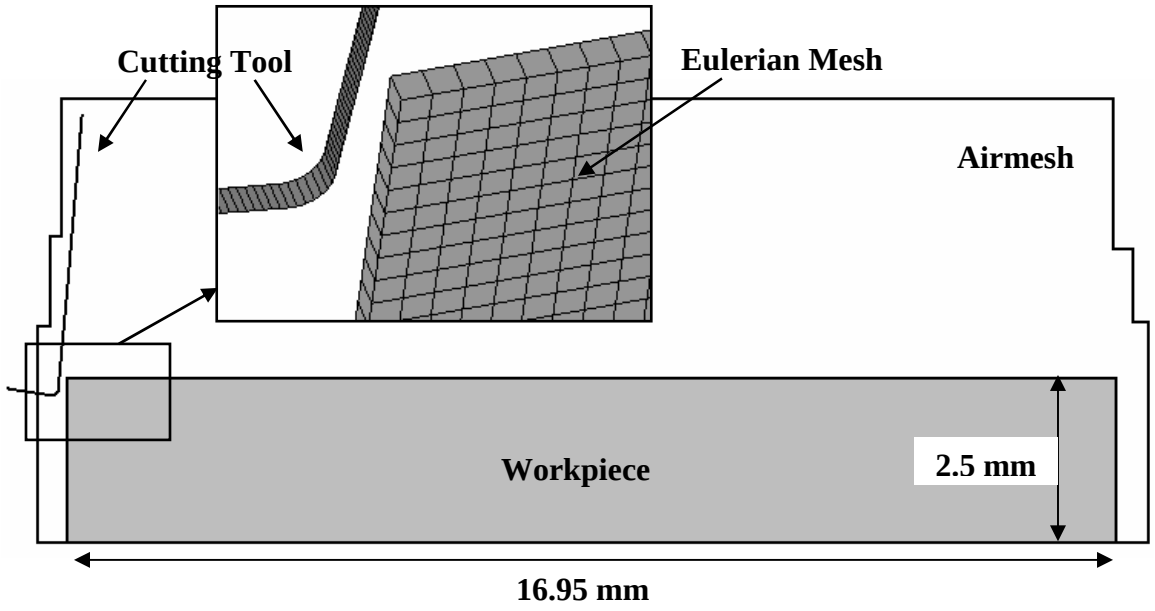

(a)

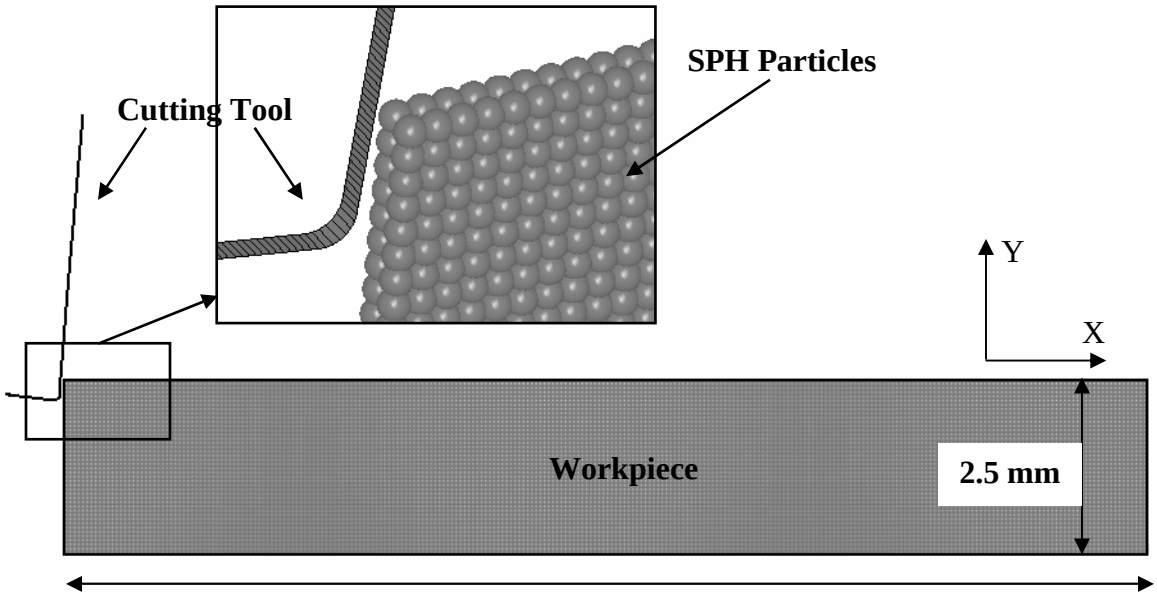

(b)

Figure 1: Schematic diagrams showing the geometry of the finite element model of the tool and the workpiece: **(a)** the Eulerian model, **(b)** the SPH.

Strain and Stress Distributions

The numerically computed strain distributions obtained from the Eulerian and SPH models in the workpiece are shown in Figures 2 (b) and (c) with the experimentally determined values presented in Figure 2 (a). The location of the maximum equivalent strain was at the tool tip at X = 0 and Y = 0 for both of the models. A maximum strain of 7.5 was obtained in the Eulerian model (Figure 2 (b)) and 8.0 at the SPH model (Figure 2 (c)) which was not possible to observe from the experimental approach (Figure 2(a)). The general trends that emerge from the distributions of the numerically predicted strain values were similar to those obtained from the experimental measurements. A strain of 0.1 was predicted at a depth of 200 μm below the cutting line for both of the models. When compared along the primary shear plane, both the experimental measurements and the numerical simulations predicted an equivalent plastic strain of 3.4 directly ahead of the tool tip (X = 100 μm, Y = 0 μm for the experimental measurements, X = 150 μm, Y = 0 μm for both of the numerical models). In the mid-section of the primary shear plane, the experimentally determined strain was 2.0, while the corresponding numerically predicted strain value was 1.95 for the Eulerian model and 1.55 for the SPH model. The thickness of the primary deformation zone (PDZ) was approximately 700 μm for the Eulerian model and 600 μm for the SPH model compared to 800 μm experimental observation. Numerical models predicted the width of the secondary deformation zone (SDZ) as 250 μm. In general, both the Eulerian and SPH models showed good overall correlation with the experimentally measured strains.

The numerically predicted stress distributions obtained from the Eulerian and SPH models using the exponential material model for the workpiece are shown in Figures 3 (b) and (c). The maximum flow stress (301 MPa) was located at the tool tip, and its location corresponded to the location of the maximum strain. The predicted maximum flow stress was 6 % higher than the experimental stress (284 MPa, Figure 3 (a)). The stresses decreased with increasing distance from the cutting line until below a certain depth where they became equal to the yield strength of the material. Along the primary shear plane, the stress decreased from the maximum value of 301 MPa to 221 MPa at the chip root for the Eulerian model and to 205 MPa for the SPH model. The stress within the chip reached values ranging from 221 MPa to 269 MPa for the Eulerian model and 205 MPa to 269 MPa for the SPH model.

Conclusions

1. Using a deformation response based on exponential-type stress-strain relationship in an SPH based FEA, stress and strain values of aluminum subjected to orthogonal machining were predicted in terms of both magnitudes and distributions. The predictions of the deformation state of the material ahead of the tool tip provided by the SPH technique were also in general agreement with those of the Eulerian technique.

2. Along the primary shear plane, the numerical simulations predicted an equivalent plastic strain of 3.4 directly ahead of the tool tip. The maximum predicted plastic strains utilizing an Eulerian and SPH solutions were 7.5 and 8.0, respectively. The experimentally determined strain was 2.0 in the mid-section of the primary shear plane, while the corresponding numerically predicted strain value was 1.95 for the Eulerian model and 1.55 for the SPH model. The thickness of the PDZ was approximately 700 μm for the Eulerian model and 600 μm for the SPH model compared to 800 μm from experimental observations.

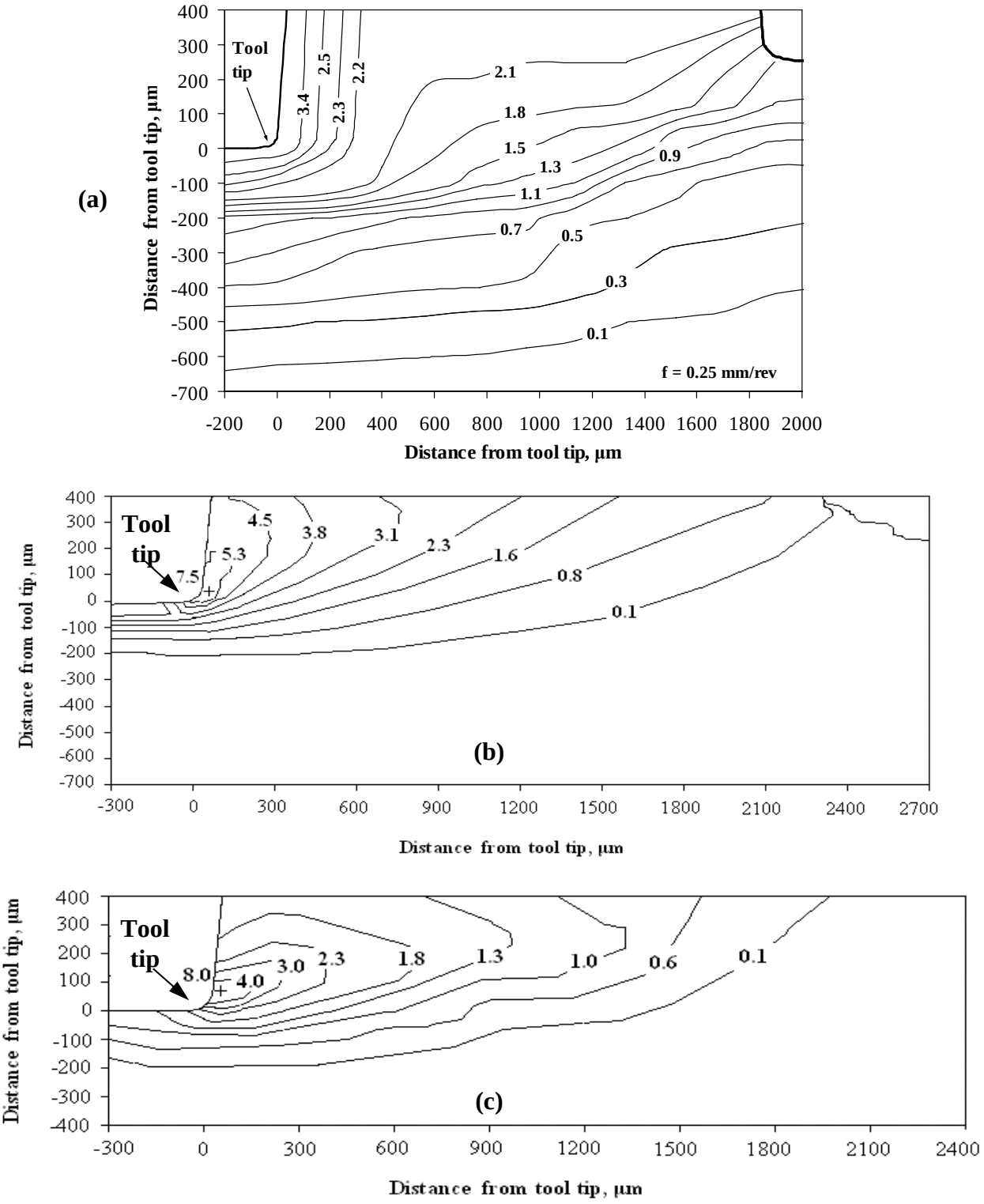

Figure 2: Experimentally and numerically determined strain distributions in the material ahead of the tool tip: **(a)** Experimental measurements, **(b)** the Eulerian model and **(c)** the SPH model.

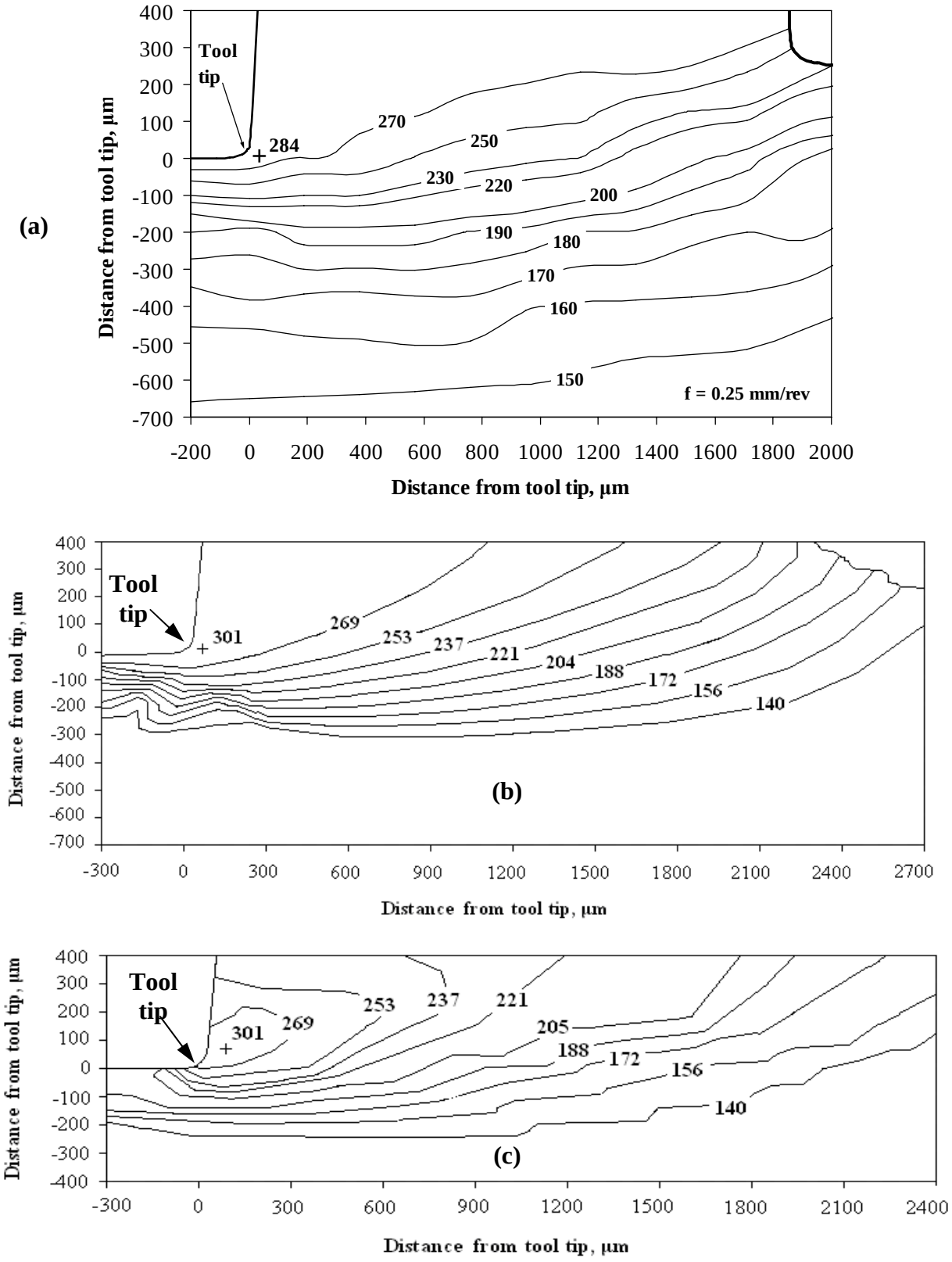

Figure 3: Experimentally determined and numerically predicted stress distributions (MPa) in the material ahead of the tool tip: **(a)** Experimental measurements, **(b)** the Eulerian model and **(c)** the SPH model.

3. When the CPU time requirements are considered, the SPH model is the suitable choice to model deformation processes during cutting with relatively good accuracy and approximately 2.75 times less cost compared to the Eulerian model.

References

[1] D. J. Benson and S. Okazawa, in: Proceedings of the 8th international Conference on Numerical Methods in Industrial Forming Processes, Columbus, 2003.
[2] D. J. Benson and S. Okazawa, Computatinal Methods in Applied Mechanics and Engineering, 193 (2004) 4277-4298.
[3] M. N. A. Nasr, E. G. Ng and M. A. Elbestawi, International Journal of Machine Tools and Manufacture, 47 (2007) 401-411.
[4] H. Migulez, R. Zaera, A. Rusinek, A. Moufki and A. Molinari, Journal de Physique IV, 134 (2006) 417-422.
[5] A. Raczy, M. Elmadagli, W. J. Altenhof and A. T. Alpas, Metallurgical and Materials Transactions A, 35 (2004) 2393-2400.
[6] J. L. Lacome, in: 6th International LS-DYNA User's Conference, Dearborn, 2000, Session 7, pp. 29-34.
[7] P. Cleary, M. Prakash, J. Ha, M. Sinnott, T. Nguyen and J. Grandfield, JOM, 56 (2004) 67-70.
[8] L. E. Schwer, in: 8th International LS-DYNA User's Conference, Dearborn, 2004, Session 8, pp. 1-12.
[9] M. Buyuk, C. D. S. Kan, N. E. Bedewi, A. Durmus and S. Utku, in: 8th International LS-DYNA User's Conference, Dearborn, 2004, Session 8, pp. 81-96.
[10] J. Limido, C. Espinosa, M. Salaun and J. L. Lacome, International Journal of Mechanical Science, 49 (2007) 898-908.
[11] LS-DYNA, Keyword User's Manual, Version 971, Livermore Software Technology Corporation, Livermore, 2006.
[12] E. Voce, Journal of Institute of Metals, 74 (1948) 537-562.
[13] D. J. Steinberg, Equation of State and Strength Properties of Selected Materials, Lawrence Livermore National Laboratory, Livermore, CA, 1996.